J. Space Weather Space Clim. 2 (2012) A05
DOI: 10.1051/swsc/2012004

SWSC

Extreme changes in the dayside ionosphere during a Carrington-type magnetic storm

Bruce T. Tsurutani[1,*], Olga P. Verkhoglyadova[1,2], Anthony J. Mannucci[1], Gurbax S. Lakhina[3], and Joseph D. Huba[4]

[1] Jet Propulsion Laboratory, California Institute of Technology, Pasadena, California, USA
*corresponding author: e-mail: bruce.tsurutani@jpl.nasa.gov
[2] CSPAR, University of Alabama, Huntsville, Alabama, USA
[3] Indian Institute of Geomagnetism, Navi Mumbai, Maharastra, India
[4] Naval Research Laboratory, Washington DC, USA

Received 9 February 2012 / Accepted 12 May 2012

ABSTRACT

It is shown that during the 30 October 2003 superstorm, dayside O^+ ions were uplifted to DMSP altitudes (~850 km). Peak densities were ~9×10^5 cm^{-3} during the magnetic storm main phase (peak Dst = −390 nT). By comparison the 1–2 September 1859 Carrington magnetic storm (peak Dst estimated at −1760 nT) was considerably stronger. We investigate the impact of this storm on the low- to mid-latitude ionosphere using a modified version of the NRL SAMI2 ionospheric code. It is found that the equatorial region (LAT = 0° ± 15°) is swept free of plasma within 15 min (or less) of storm onset. The plasma is swept to higher altitudes and higher latitudes due to E × B convection associated with the prompt penetration electric field. Equatorial Ionization Anomaly (EIA) O^+ density enhancements are found to be located within the broad range of latitudes ~ ± (25°–40°) at ~500–900 km altitudes. Densities within these peaks are ~6×10^6 oxygen ions-cm^{-3} at ~700 km altitude, approximately +600% quiet time values. The oxygen ions at the top portions (850–1000 km) of uplifted EIAs will cause strong low-altitude satellite drag. Calculations are currently being performed on possible uplift of oxygen neutrals by ion-neutral coupling to understand if there might be further significant satellite drag forces present.

Key words. ionosphere (equatorial) – ionosphere (mid latitude) – electric field – coronal mass ejection (CME) – flares

1. Introduction

Obayashi (1967), Nishida (1968), and Kelley et al. (1979, 2003) have reported strong ionospheric effects associated with magnetospheric substorms. These effects are explained by the appearance of dawn-to-dusk electric fields in the dayside near-equatorial ionosphere which has received the name "prompt penetrating electric fields" or PPEFs. More recently, such strong ionospheric effects have been noted during magnetic storms (Sobral et al. 1997, 2001; Sastri et al. 2002; Tsurutani et al. 2004, 2008a, 2008b; Huang et al. 2005; Mannucci et al. 2005, 2008; Koga et al. 2011; Siqueira et al. 2011). The importance of the latter is that during storms, the electric fields are more intense (Tsurutani et al. 2004) and have longer durations up to hours (Huang et al. 2005). The ionospheric effects during storms would thus be expected to be stronger and more prominent.

These PPEFs may be one and the same as the magnetospheric convection electric fields that drive the nightside plasmasheet into the inner magnetosphere, creating the ring current during magnetic storms (Tsurutani et al. 2004). For the interested reader, intense magnetic storms have been discussed in Tsurutani et al. (1988, 1992, 2008a), Gonzalez et al. (1994, 2011), and Echer et al. (2008a, 2008b). For a more detailed discussion of the relationship between PPEFs and magnetic storms, we refer the reader to Tsurutani et al. (2008b).

The cause for an increase in the total electron content (TEC) during magnetic storm main phases has been explained in Tsurutani et al. (2004). During a magnetic storm when the PPEF reaches the equatorial dayside ionosphere, the E × B convection uplifts ionospheric plasma to greater heights and (absolute) magnetic latitudes. At these greater heights, the recombination time scale is considerably longer than at lower altitudes. Solar photoionization creates new electron-ion pairs at the lower heights, replenishing the displaced plasma. Thus, the overall TEC of the ionosphere increases. This process has been called the "dayside ionospheric superfountain" (Mannucci et al. 2005; Tsurutani et al. 2008b) and is one type of a "positive ionospheric storm" (Prölss 1993).

Although the 30–31 October 2003 storm was intense (peak Dst = −390 nT), the 1–2 September 1859 Carrington event was far more intense. Tsurutani et al. (2003) and Lakhina et al. (2012) used the Colaba, India magnetometer data, the Carrington solar flare and magnetic storm timing and other ancillary information to determine the Dst of the event to be ~ −1760 nT, over four times the intensity of the October 2003 storm and more than three times the intensity of the 13 March 1989 Quebec, Canada storm. The latter storm knocked out the Hydro-Quebec power grid for ~9 h.

Because of this great intensity, the Carrington storm (the authors pay tribute to R. Carrington by naming it after him) had related effects that influenced humankind. At the time, telegraph communication was the "high technology" of the era. The magnetic storm induced currents in the east-west lying telegraph lines such that arcing caused fires at telegraph stations in both the United States and Europe (Loomis 1861). It is realized that if such an intense storm occurred today, similar induced

currents would occur in our power (and other) lines (Bolduc 2002). NASA, the Department of Defense, and Homeland Security are investigating the possibility of major power grid failures if such a magnetic storm occurred today.

Are there other problems that can occur in our high-tech society due to the occurrence of such storms? The purpose of this paper is to study the gross properties of the ionosphere during a Carrington-type storm.

2. Methods of analyses

We will explore the dayside ionospheric perturbations using the SAMI2 code (Huba et al. 2000, 2002). SAMI2 is a low-latitude ionospheric model which describes dynamics and chemical evolution of seven ion species and seven corresponding neutral species. The code solves collisional two-fluid equations for electrons and ions along the Earth's dipole magnetic field lines, taking into account photoionization of neutrals, recombination of ions and electrons, and chemical reactions. The code was modified to allow an electric field input (Verkhoglyadova et al. 2007) and more recently (for this paper) has been further modified to insert 3-h Ap indices instead of daily values.

The SAMI2 code calculates ionospheric plasma transport in a direction perpendicular to the ambient magnetic field lines. Diurnal variations are associated with a variable electric field, which we have assumed has a sinusoidal shape in the form $\sin[(t - 7)/24]$ where t is the time in local time hours. We take a peak field of 0.53 mV m^{-1} electric field in the dawn-dusk direction (Huba et al. 2000).

The ionospheric electric field for the Carrington storm was obtained from Tsurutani et al. (2003), a value of 20 mV m^{-1} in the dawn-dusk direction. This enhanced ionospheric electric field was superposed on top of the diurnal field and was applied at 1200 LT and terminated at 1300 LT, in basic agreement with the observation of the storm main phase duration (Tsurutani et al. 2003).

3. Results

3.1. 30–31 October 2003 superstorm event

Figure 1 shows the DMSP data for oxygen ions during the 30–31 October 2003 superstorm. We emphasize that the PPEF will uplift the dayside ionospheric ions as well as electrons keeping the plasma neutral. Since different ion species will have different initial altitude profiles, their altered storm-time profiles will be different from each other as well. On the other hand, they will all have the same general uplift to higher altitudes and absolute latitudes caused by the convection PPEFs.

We show an example of ionospheric ion uplift during the 30 October 2003 magnetic storm. The top panel contains a pass prior to the uplift, from 1750 to 1820 UT. DMSP flew at a constant altitude of ~850 km and crossed the magnetic equator at ~1804 UT at ~0940 LT (late morning). A single peak ion density with an intensity of $\sim 1.5 \times 10^5$ cm^{-3} is recorded. This peak is estimated to contain 95% oxygen ions. According to Mannucci et al. (2005), this measurement was taken at the end of the magnetic storm recovery phase of the storm that preceded the 30 October event.

The bottom panel of Figure 1 shows the interval between 1930 and 2000 UT 30 October 2003. This interval is in the middle of the developing main phase of the 30–31 October

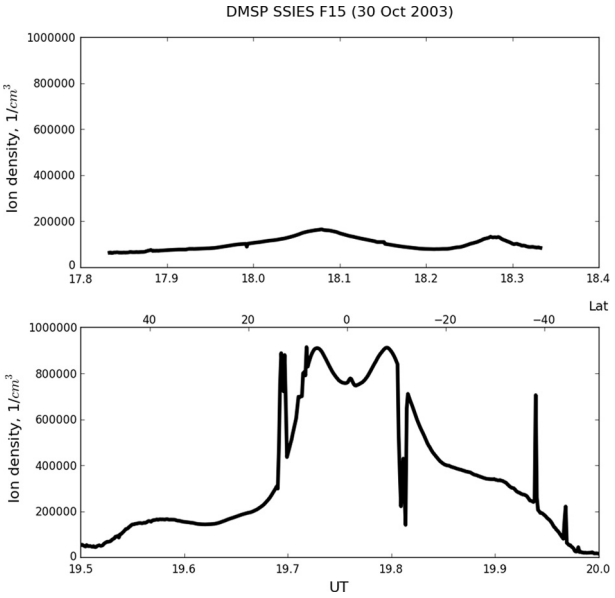

Fig. 1. Oxygen ion densities for two DMSP F15 passes across the dayside ionosphere during 30 October 2003.

2003 storm. A remarkable feature is the very large oxygen ion (99%) enhancements near the equator. The dual peaks are noted at ±8° on either side of the equator, with peak densities of ~9 × 10^5 cm^{-3}. Thus in the time of one orbital pass (~90 min), the peak densities at ~850 km altitude have increased by ~600%. We presume that this is due to the PPEFs associated with the magnetic storm.

There are some sharp enhancements and depletions noted in the bottom panel of the figure. There is a sharp increase at ~1941 UT when the satellite crossed ~15° LAT and a sharp depression at ~1949 UT when the satellite was at −12° LAT. Although it is unclear whether these features are spatial or temporal, it can be argued that they are spatial if one notes that they occur at approximately the same absolute latitude location. These enhancements/depressions are most likely "plasma bubbles". A density enhancement in one hemisphere may lead to a depletion in the other (as can be noted above). The bubbles may be associated with a Rayleigh-Taylor instability associated with the rapid plasma uplift process.

Figure 2, taken from Mannucci et al. (2005), displays verticalized TEC data from the CHAMP spacecraft which was orbiting the Earth at an altitude of ~400 km. CHAMP only detects the part of the ionosphere that is above the satellite. Three orbits from ~ ±60° MLAT are shown. The blue curve shows a quiet time TEC distribution prior to the superstorm on 30 October 2003. The normal equatorial ionospheric anomalies (EIAs; Namba & Maeda 1939; Appleton 1946) are present at ~ ±10°. The next two curves in red and black correspond to the TEC above CHAMP after the magnetic storm had started and was in progression, respectively. In the beginning of the magnetic storm (red curve), the EIAs are now located at ~ ±22° LAT with peak TEC values of ~210 units.

The third pass is the most dramatic of all. The black curve shows that the ionospheric anomalies have moved to higher magnetic latitudes and are even more intense. The peaks are now at ~ ±30° and have values of ~270 TEC units in the northern hemisphere and ~330 TEC units in the southern

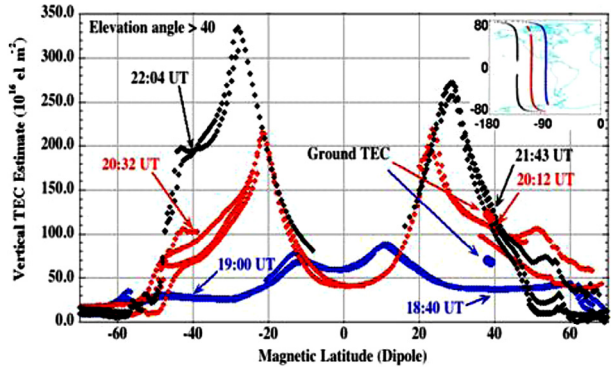

Fig. 2. Three passes of the CHAMP satellite through the dayside ionosphere at ~1230–1330 LT. CHAMP was at an altitude of ~400 km. The blue curve was taken prior to the 30 October 2003 magnetic storm. The red curve was taken at the beginning of the storm, and the black near the end of the storm. The figure is taken from Mannucci et al. (2005), Figure 3.

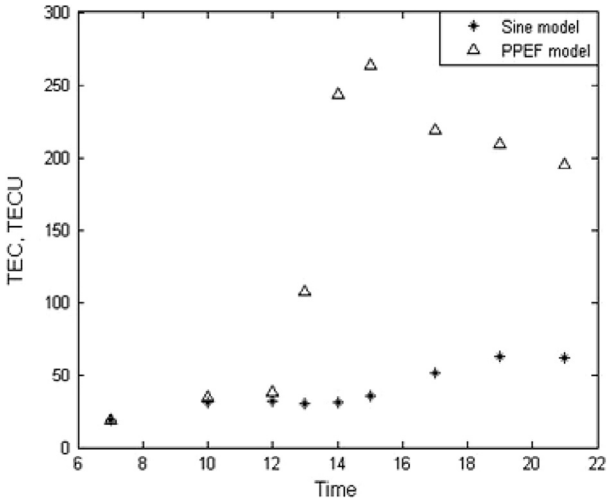

Fig. 3. The SAMI2-derived TEC at altitudes above 400 km at ~1300 LT and at 25° LAT. The starred values are for a quiet time interval with a peak diurnal electric field of 0.53 mV m^{-1} at 13 LT. The open triangles represent the TEC for the case of an electric field of 4 mV m^{-1} for a 2 h duration. In the storm case, the TEC increases until a peak value of ~270 TEC units is reached. This closely matches the peak EIA observed by CHAMP.

hemisphere. The southern hemispheric peak may be higher either due to the fact that the spacecraft passed through the south peak later in time or this could be a seasonal effect.

3.2. The accuracy of the SAMI2 model

It would be useful to first make some comments about the accuracy and reproduction of the data by the SAMI2 code. To apply the SAMI code, the PPEF for 30 October 2003 was first calculated following the Rostogi & Klobuchar (1990) technique using the CHAMP scalar magnetometer measurements of the equatorial electrojet (EEJ) during the storm. The Kyoto University ionospheric model was used to obtain the conductivity values. The EEJ was assumed be centered at an altitude of 105 km, where a Cowling conductivity of 1.9×10^{-2} Sm^{-1} was calculated for local noon. The magnetic perturbation at the CHAMP was measured, a ground reflectance of ~11% and an infinite line current assumed in order to derive the electric field intensity. A value of ~4 mV m^{-1} was obtained. We direct the reader to the original articles (Verkhoglyadova et al. 2007, 2008; Tsurutani et al. 2008b) for more details.

How do the SAMI2 model results compare with the Mannucci et al. (2005) TEC measurements? The TEC at altitudes above 400 km at ~1300 LT and at 25° LAT have been calculated and are shown in Figure 3. Two curves are displayed, a quiet time set of values shown in stars and the 30 October 2003 storm interval (with 2 h of E = 4 mV m^{-1} applied) shown in open triangles. In the storm electric field case, the TEC increases until ~1515 LT when a peak value of ~270 TEC units is reached. This closely matches the peak EIA observed by CHAMP during the third CHAMP pass shown in Figure 2. This also suggests that the very large electric field values derived using the CHAMP magnetometer measurements are quite plausible.

From the use of the SAMI2 model which has no disturbance winds included, it is shown that the features of the peaks in the anomalies can be explained by the PPEF alone. Most if not all of the peak TEC intensities are caused by the PPEFs during the first 2 h of the intense magnetic storm (not shown to save space).

Although an exact comparison between SAMI2 modeling and the CHAMP data cannot be made, we believe the above results show excellent agreement in general.

3.3. Modeling the Carrington storm event

For the Carrington storm event, we are not able to measure the electric field imposed on the EEJ. However, we do have an estimate of the electric field and its duration for the magnetic storm based on other data (Tsurutani et al. 2003). A 20 mV m^{-1} electric field for a duration of 1 h will be assumed.

The 3-h Ap inputs used for the SAMI2 code prior to and during the superstorm were 50, 70, 150, 400 (storm onset), 400, 350, 300, and 200 nT. These values had only minor effects on the ionospheric response, so they are not too critical.

Figure 4a shows the quiet time ionospheric electron densities for the 1–2 September 1859 storm. The two EIAs are noted, one spanning ~ −10° to −30° LAT and a second from ~ +5° to +25° LAT (we use 3.25×10^6 electrons-cm^{-3} as the threshold for the regions). The altitudes of the two EIAs are a bit different. The southern hemisphere ionization enhancement spans ~300–520 km, while the northern hemisphere one is located from ~270–410 km.

The dayside ionosphere 30 min after the PPEF has been applied is shown in Figure 4b. The equatorial region between −10° and +20° LAT is almost devoid of plasma (~$0.5–1 \times 10^6$ electrons-cm^{-3}). Due to the E × B convection, the dense plasma is now located at higher latitudes and altitudes and has greater intensities. The southern hemispheric peak spans ~ −15° to −35° LAT and the northern hemispheric peak is located at ~ +25° to +35° LAT. The peak densities of ~3.25×10^6 electrons-cm^{-3} range from ~500 to 900 km altitude.

The EIAs 1 h after the PPEF has been applied are shown in Figure 4c. The electron densities are now much larger than the previous panel by almost a factor of 2. The peak values are now ~5.5×10^6 electrons-cm^{-3}. Using a value of 3.25×10^6 electrons/cm^{-3} to define the enhancements as was done with the prior figures, the EIA peaks are located at ~510–910 km and ~530–900 km for the southern and northern regions, respectively. The magnetic latitude ranges are now ~ −15° to −40° LAT and ~ +30° to +45° LAT.

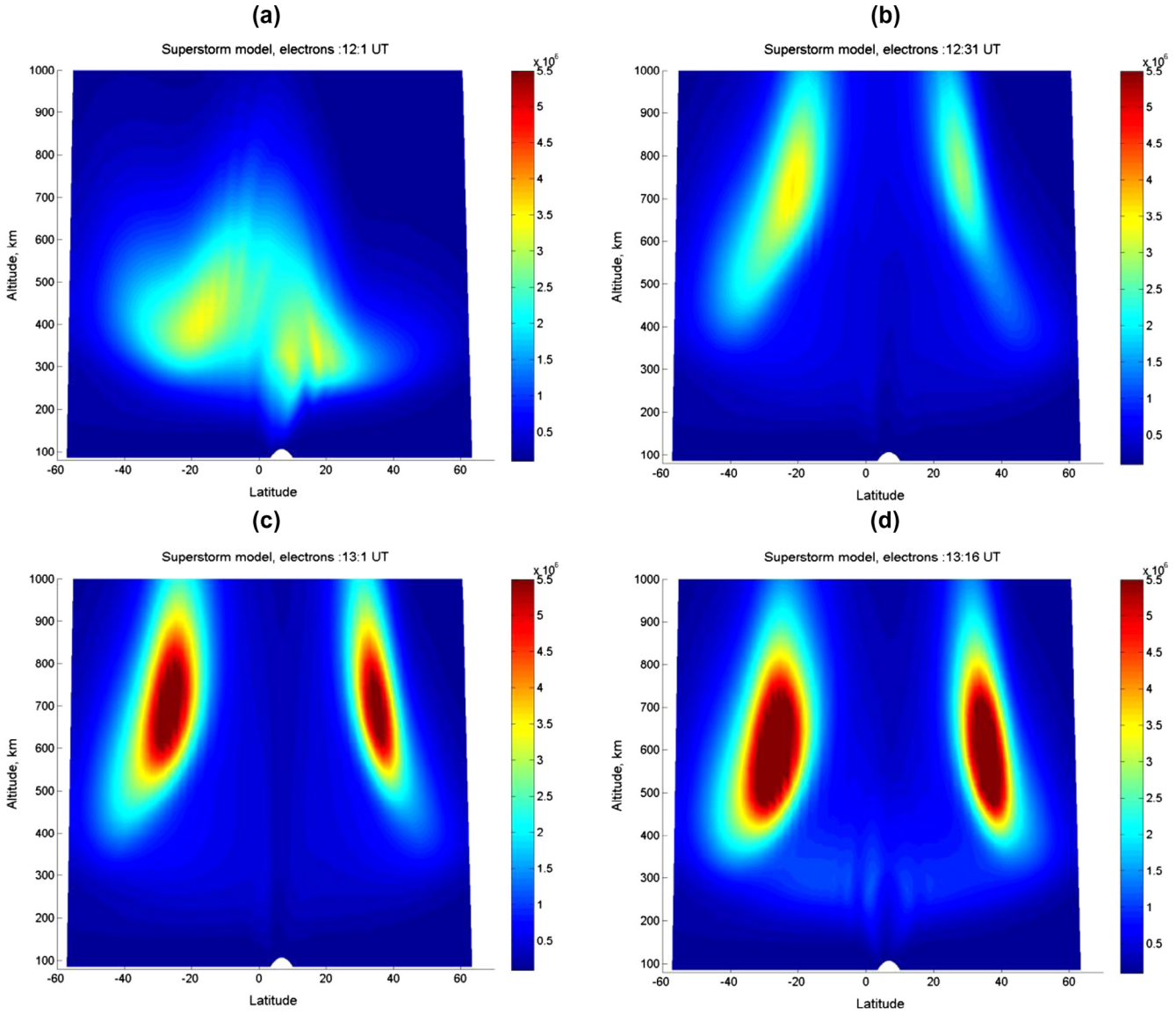

Fig. 4. The EIA electron anomalies: (a) prior to, (b) 30 min after onset of the PPEF, (c) 1 h after onset of the PPEF, and (d) 15 min after termination of the PPEF.

One final panel is shown for completeness. Figure 4d shows the ionosphere 15 min after the storm electric field was terminated. Two major differences from Figure 3 should be noted. The equatorial region has now recovered somewhat due to photoionization and a lack of convection to higher altitudes. The densities are now ~1.5×10^6 electrons-cm^{-3} instead of ~0.5×10^6 electrons-cm^{-3}. The EIA peaks are now located at ~ −15° to −40° LAT and ~400–820 km for the southern peak and ~ +30° to +45° LAT and ~400–820 km for the northern peak. The peaks have descended ~100 km in the 15 min time span.

The oxygen dynamics during the 1859 storm simulation is shown in Figure 5. The four panels represent the same cases: (a) prior to the PPEF application, (b) 15 min after application, (c) 1 h after application, and (d) 15 min after the PPEF was terminated. The sequence of the events looks similar to that of the electrons. However, we note that not all ions have the same altitude profiles. The NO^+ ions show considerably different uplift dynamics, but will not be shown here to conserve space.

In panel (a) the equatorial region from ~ −15° to +20° LAT is devoid of O^+ ions with a background level of 2.5×10^6 cm^{-3}. Using a threshold of 3.5×10^6 cm^{-3} O^+ density, the southern hemispheric anomaly is located at ~ −5° to −30° LAT and ~300–500 km altitude and ~5°–20° LAT and ~280–430 km altitude for the northern hemispheric anomaly. The asymmetry of the two anomalies is essentially the same as was shown for the electrons.

For panel (b) using the same threshold as above (~3.5×10^6 cm^{-3}), the southern hemispheric anomaly is located at ~ −15° to −35° LAT and ~550 to 850 km altitude and ~25°–35° LAT and ~650–850 km altitude for the northern hemispheric anomaly.

Panel (c) gives the O^+ densities 1 h after the PPEFs have been applied. The southern hemispheric anomaly is located at ~ −20° to −35° LAT and ~530–920 km altitude and ~30°–45° LAT and ~500–900 km altitude for the northern hemispheric anomaly. The peak values reach ~6×10^6 O^+ cm^{-3} at altitudes centered at ~700 km. It is noted that the densities of the uplifted EIA peaks at 850 km and 1000 km were ~4×10^6 cm^{-3} and ~3.5×10^6 cm^{-3}, respectively. What is interesting about these ion densities is that they are substantially above quiet time neutral densities, about ~40 times at 850 km and ~300 times at 1000 km.

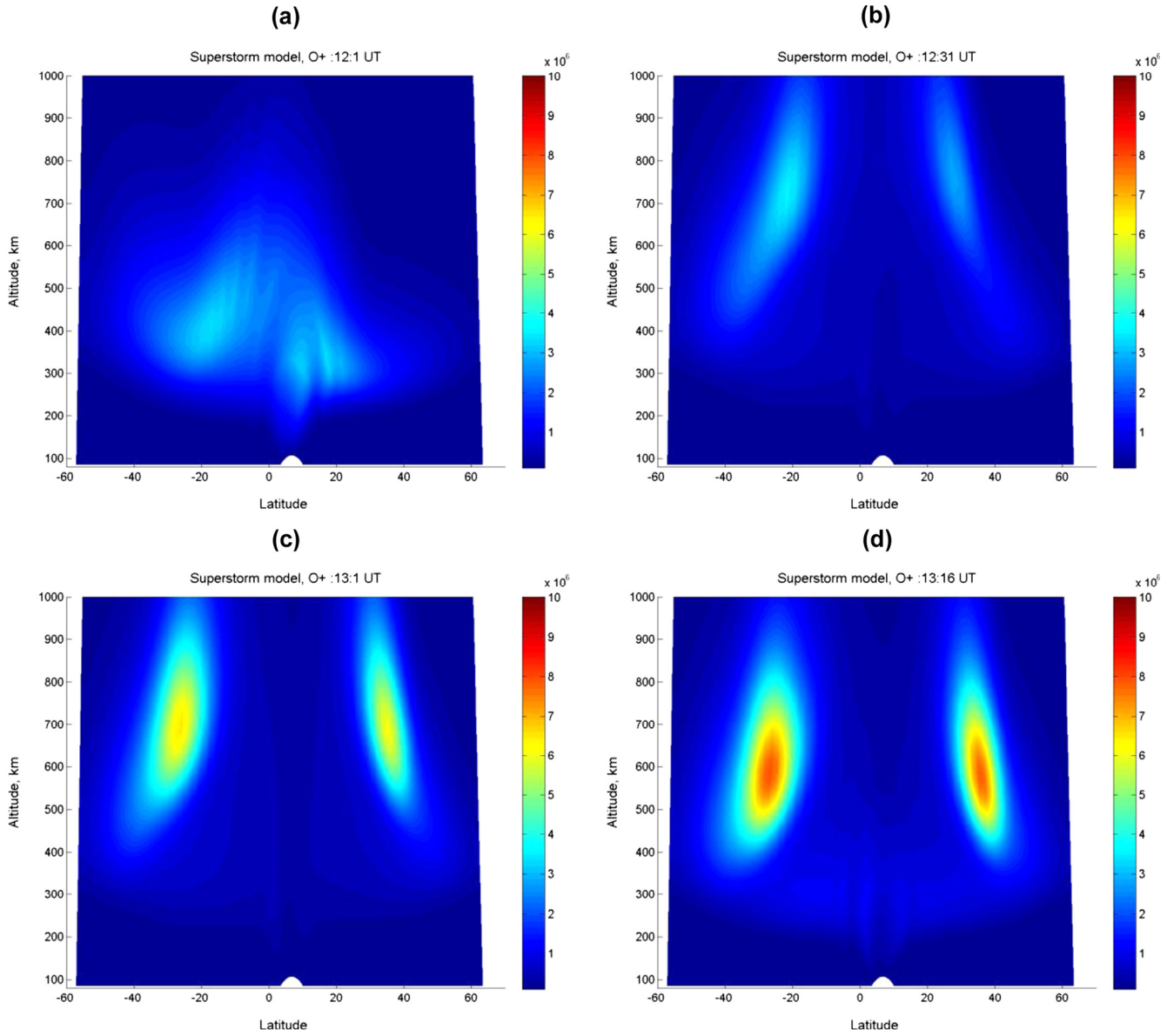

Fig. 5. The oxygen ion dynamics during the 1859 storm simulation. The general format is the same as for Figure 4.

The anomalies have density increases after the storm is over (panel d). Peak densities of 7–8 × 10^6 cm^{-3} are noted at ~600 km altitude 15 min after storm/PPEF termination. The southern hemispheric anomaly is located at ~ −15° to −35° LAT and ~400–830 km altitude and ~30°–45° LAT and ~400–800 km altitude for the northern hemispheric anomaly.

4. Summary and conclusions

The modified SAMI2 code has been run to simulate the conditions during a Carrington-type magnetic storm. The equatorial region is swept clean of plasma within 15 min of application of the storm-time electric field (within the view of the simulation). The EIAs are even more prominent and are found at higher altitudes and higher latitudes. The ionosphere is quite dynamic during the storm main phase (PPEF input). However, intense plasma densities are noted ~1 h into the storm main phase. EIA/Appleton anomaly O^+ peaks are located at ~ −20° to −35° LAT and ~500–900 km for the southern peak and +30° to +45° LAT and ~520–900 km for the northern peak, respectively.

The rapid ionospheric uplift may possibly lead to instabilities which could lead to "plasma density bubbles" (Keskinen et al. 1981; Ossakow 1981). If the latter occurs, GPS receivers below this portion of the ionosphere could be disrupted for the storm duration and perhaps longer. The density gradients themselves (without instabilities) may be sufficient to disrupt GPS links. Modeling is needed to study this possible effect.

The rapid upward convection of oxygen ions will lead to some level of oxygen neutral uplift due to ion-neutral collisions (see Tsurutani et al. 2007). Calculations are presently being done in a companion paper (Lakhina et al. 2012). It is possible that severe satellite drag could be a consequence of this latter effect.

5. Final comments

We note that such extreme ionospheric effects as those that have been simulated in this paper have never been observed in spacecraft or remote sensing ground instrumentation. We speculate that it is because we have not experienced a magnetic storm

with Carrington-level intensities during the space age. On the other hand, Loomis (1861) has well documented the fires set by induced potentials in telegraph lines during the Carrington magnetic storm and thus we conclude that extreme electric fields such as simulated here can and do occur. Increased awareness and call for preparedness for an extreme space storm were expressed recently by Hapgood (2012).

What are the consequences of the extremely rapid uplift of the ionosphere? One feature mentioned in the text is that plasma instabilities such as Rayleigh-Taylor may occur, leading to the generation of "plasma bubbles", regions of strong electron density gradients. These will disrupt GPS communications. Future ionospheric modeling will tell us how severe this effect may be and for what duration this phenomenon will be effective. A second feature is that the uplift of high latitude portions of the EIAs to ~850 and 1000 km altitude will increase satellite drag substantially. A third possible consequence is strong ion-neutral drag which will increase the neutral atom densities at >800 km altitudes. However to obtain a more thorough understanding of the nature of this effect, a computer subroutine that self-consistently solves the neutral atom continuity and momentum equations in the presence of ion-neutral drag forces needs to be developed. This code could then be applied to this case and cases like it. As was noted in the simulation results, the ionosphere is highly dynamic during such an extreme magnetic storm, and one should not think of it as being in an equilibrium state. Even in the storm decay phase, the ionosphere and upper atmosphere may be changing rapidly.

Acknowledgements. Portions of this research effort were performed at the Jet Propulsion Laboratory, California Institute of Technology under contract with the NASA. GSL thanks the Indian National Science Academy, New Delhi for support under the Senior Scientist Scheme. JDH thanks NRL 6.1 Base Funds for support of this research. We gratefully acknowledge the Center for Space Sciences at the University of Texas at Dallas and the U.S. Air Force for providing the DMSP thermal plasma data.

References

Appleton, E.V., Two anomalies in the ionosphere, *Nature*, **157**, 691, 1946.

Bolduc, L., GIC observations and studies in the Hydro-Quebec power system, *J. Atmos. Sol. Terr. Phys.*, **64**, 1793, 2002.

Carrington, R.C., Description of a singular appearance seen in the Sun on September 1, 1859, *Mon. Not. R. Astron. Soc.*, **20**, 13, 1859.

Echer, E., W.D. Gonzalez, and B.T. Tsurutani, Interplanetary conditions leading to superintense geomagnetic storms (Dst < −250 nT) during solar cycle 23, *Geophys. Res. Lett.*, **35**, L06S03, DOI: 10.1029/2007GL03175, 2008a.

Echer, E., W.D. Gonzalez, B.T. Tsurutani, and A.L.C. Gonzalez, Interplanetary conditions causing intense geomagnetic storms (Dst < −100 nT) during solar cycle 23 (1996–2006), *J. Geophys. Res.*, **113**, A05221, DOI: 10.1029/2007JA012744, 2008b.

Gonzalez, W.D., E. Echer, A.L. Clua de Gonzalez, B.T. Tsurutani, and G.S. Lakhina, Extreme geomagnetic storms, recent Gleissberg cycles and space era-superintense storms, *J. Atmos. Sol. Terr. Phys.*, **73**, 1447, 2011.

Gonzalez, W.D., J.A. Joselyn, Y. Kamide, H.W. Kroehl, G. Rostoker, B.T. Tsurutani, and V.M. Vasyliunas, What is a geomagnetic storm?, *J. Geophys. Res.*, **99 (A4)**, 5771, 1994.

Hapgood, M., Prepare for the coming space weather storm, *Nature*, **484**, 311, 2012.

Hodgson, R., On a curious appearance seen in the Sun, *Mon. Not. R. Astron. Soc.*, **20**, 15, 1859.

Huang, C.-S., J.C. Foster, and M.C. Kelley, Long-duration penetration of the interplanetary electric field to the low-latitude ionosphere during the main phase of magnetic storms, *J. Geophys. Res.*, **110**, A11309, DOI: 10.1029/2005JA011202, 2005.

Huba, J.D., K.F. Dymond, G. Joyce, S.A. Budzien, S.E. Thonnard, J.A. Fedder, and R.P. McCoy, Comparison of O^+ density from ARGOS LORAAS data analysis and SAMI2 model results, *Geophys. Res. Lett.*, **29 (7)**, 6-1, DOI: 10.1029/2001GL013089, 2002.

Huba, J.D., G. Joyce, and J.A. Fedder, Sami2 is another model of the ionosphere (SAMI2): A new low-latitude ionosphere model, *J. Geophys. Res.*, **105 (A10)**, 23035, 2000.

Kelley, M.C., B.G. Fejer, and C.A. Gonzales, An explanation for anomalous equatorial ionospheric electric field associated with a northward turning of the interplanetary magnetic field, *Geophys. Res. Lett.*, **6 (4)**, 301, 1979.

Kelley, M.C., J.J. Makela, J.L. Chau, and M.J. Nicolls, Penetration of the solar wind electric field into the magnetosphere/ionosphere system, *Geophys. Res. Lett.*, **30 (4)**, 1158, 2003.

Keskinen, M.J., E.P. Szuszczewicz, S.L. Ossakow, and J.C. Holmes, Nonlinear theory and experimental observations of the local collisional Rayleigh-Taylor instability in a descending equatorial spread F ionosphere, *J. Geophys. Res.*, **86 (A7)**, 5785, 1981.

Koga, D., J.H.A. Sobral, W.D. Gonzalez, D.C.S. Arruda, M.A. Abdu, et al., Electrodynamic coupling processes between the magnetosphere and the equatorial ionosphere during a 5-day HILDCAA event, *J. Atmos. Sol. Terr. Phys.*, **73**, 148, 2011.

Lakhina, G.S., S. Alex, B.T. Tsurutani, and W.D. Gonzalez, Super magnetic storms: Hazzard to society, in *Complexities and Extreme Events in Geosciences*, eds. A.S. Sharma, A. Bunde, D. Baker, and V.P. Dimri, Geophysical Monograph Series, American Geophysical Union Press, Washington DC, 2012, in press.

Loomis, E., On the great auroral exhibition of Aug. 28th to Sept. 4, 1859, and on auroras generally, *Am. J. Sci.*, **82**, 318, 1861.

Mannucci, A.J., B.T. Tsurutani, M.A. Abdu, W.D. Gonzalez, A. Komjathy, E. Echer, B.A. Iijima, G. Crowley, and D. Anderson, Superposed epoch analysis of the dayside ionospheric response to four intense geomagnetic storms, *J. Geophys. Res.*, **113**, A00A02, DOI: 10.1029/2007HA012732, 2008.

Mannucci, A.J., B.T. Tsurutani, B.A. Iijima, A. Komjathy, A. Saito, W.D. Gonzalez, F.L. Guarnieri, J.U. Kozyra, and R. Skoug, Dayside global ionospheric response to the major interplanetary events of October 29-30 2003 "Halloween storms", *Geophys. Res. Lett.*, **32**, L12S02, DOI: 10.1029/2004GL021467, 2005.

Namba, S., and K.-I. Maeda, *Maeda, Radio Wave Propagation*, Corona, Tokyo, p. 86, 1939.

Nishida, A., Coherence of geomagnetic DP2 fluctuations with interplanetary magnetic variations, *J. Geophys. Res.*, **73**, 5549, 1968.

Obayashi, T., The interaction of solar plasma with geomagnetic field, disturbed conditions, in *Solar Terrestrial Physics*, eds. J.W. King and W.S. Newman, Academic Press, London, 107, 1967.

Ossakow, S.L., Spread-F theories-a review, *J. Atmos. Terr. Phys.*, **43**, 437, 1981.

Prölss, G.W., Common origin of positive ionospheric storms at middle latitudes and the geomagnetic activity effect at low latitudes, *J. Geophys. Res.*, **98**, 5981, 1993.

Rostogi, R.G. and J.A. Klobuchar, Ionospheric electron content within the equatorial F2 layer anomaly belt, *J. Geophys. Res.*, **95**, 19045, 1990.

Sastri, J.H., K. Niranjan, and K.S.V. Subbarao, Response of the equatorial ionosphere in the Indian (midnight) sector to the severe magnetic storm of July 15, 2000, *Geophys. Res. Lett.*, **29**, 13, DOI: 10.1029/2002GL015133, 2002.

Siqueira, P.M., E.R. de Paula, M.T.A.H. Muella, L.F.C. Rezende, M.A. Abdu, and W.D. Gonzalez, Storm-time total electron content and its response to penetration electric fields over South America, *Ann. Geophys.*, **29**, 1765, 2011.

Sobral, J.H.A., M.A. Abdu, W.D. Gonzalez, W.D. Gonzalez, I. Batista, and A.L. Clua de Gonzalez, Low-latitude ionospheric response during intense magnetic storms at solar maximum, *J. Geophys. Res.*, **102**, 14305, 1997.

Sobral, J.H.A., M.A. Abdu, W.D. Gonzalez, C.S. Yamashita, A.L. Clua de Gonzalez, I. Batista, and C.J. Zamlutti, Responses of the

low latitude ionosphere to very intense geomagnetic storms, *J. Atmos. Sol. Terr. Phys.*, **63**, 965, 2001.

Tsurutani, B.T., E. Echer, F.L. Guarnieri, and O.P. Verkhoglyadova, Interplanetary causes of middle latitude ionospheric disturbances, in *Midlatitude Ionospheric Dynamics and Disturbances*, eds. P. Kintner et al., Geophysical Monograph Series, American Geophysical Union Press, Washington DC, **181**, 99, 2008a.

Tsurutani, B.T., W.D. Gonzalez, G.S. Lakhina, and S. Alex, The extreme magnetic storm of 1–2 September 1859, *J. Geophys. Res.*, **108 (A7)**, DOI: 10.1029/2002JA009504, 2003.

Tsurutani, B.T., W.D. Gonzalez, F. Tang, S.-I. Akasofu, and E.J. Smith, Origin of interplanetary southward magnetic fields responsible for major magnetic storms near solar maximum (1978–1979), *J. Geophys. Res.*, **93**, 8519, 1988.

Tsurutani, B.T., W.D. Gonzalez, F. Tang, and Y.T. Lee, Great magnetic storms, *Geophys. Res. Lett.*, **19**, 73, 1992.

Tsurutani, B.T., A. Mannucci, B. Iijima, M.A. Abdu, J.H.A. Sobral, et al., Global dayside ionospheric uplift and enhancement associated with interplanetary electric fields, *J. Geophys. Res.*, A08302, DOI: 10.1029/2003JA010342, 2004.

Tsurutani, B.T., O.P. Verkhoglyadova, A.J. Mannucci, T. Araki, A. Saito, T. Tsuda, and K. Yumoto, Oxygen ion uplift and satellite drag effects during the 30 October 2003 daytime superfountain event, *Ann. Geophys.*, **25**, 1, 2007.

Tsurutani, B.T., O.P. Verkhoglyadova, A.J. Mannucci, A. Saito, T. Araki, et al., Prompt penetration electric fields (PPEFs) and their ionospheric effects during the great magnetic storm of 30–32 October 2003, *J. Geophys. Res.*, **113**, A05311, DOI: 10.1029/2007JA012879, 2008b.

Verkhoglyadova, O.P., B.T. Tsurutani, and A.J. Mannucci, Modeling of time development of TEC variations during a superstorm event, eds. A. Bhardwaj, M. Duldig, and M. Duldig, *Adv. Geosci.*, **112**, 2007.

Verkhoglyadova, O.P., B.T. Tsurutani, A.J. Mannucci, A. Saito, T. Araki, D. Anderson, M. Abdu, and J.H.A. Sobral, Simulation of PPEF effects in dayside low-latitude ionosphere for the October 30, 2003 superstorm, in *Midlatitude Ionospheric Dynamics and Disturbances*, eds. P. Kintner, A. Coster, T. Fuller-Rowell, A. Mannucci, M. Mendillo, and R. Heelis, **169**, 181, 2008.